NIH Public Access
Author Manuscript
Stroke. Author manuscript; available in PMC 2014 January 08.

Published in final edited form as:
Stroke. 2013 August ; 44(8): . doi:10.1161/STROKEAHA.113.000903.

Spatiotemporal Uptake Characteristics of [^{18}]F-2-Fluoro-2-Deoxy-D-Glucose in a Rat Middle Cerebral Artery Occlusion Model

Hong Yuan, PhD, **Jonathan E. Frank, MS**, **Yonglong Hong, MD**, **Hongyu An, DSc**, **Cihat Eldeniz, BS**, **Jingxin Nie, PhD**, **Adomas Bunevicius, MD, PhD**, **Dinggang Shen, PhD**, and **Weili Lin, PhD**
Departments of Radiology (H.Y., H.A., J.N., D.S., W.L.) and Biomedical Engineering (C.E., W.L.), Biomedical Research Imaging Center (H.Y., J.E.F., Y.H., H.A., J.N., A.B., D.S., W.L.), University of North Carolina at Chapel Hill, NC

Abstract

Background and Purpose—Alterations of cerebral glucose metabolism are well anticipated during cerebral ischemia. However, detailed spatiotemporal characteristics of disturbed cerebral glucose metabolism during acute ischemia remain largely elusive. This study aims to delineate spatiotemporal distributions of [^{18}]F-2-fluoro-2-deoxy-D-glucose (FDG) uptake using positron emission tomography imaging, particularly at the peri-ischemic zone, and its correlation with tissue outcome.

Methods—The intraluminal suture middle cerebral artery occlusion model was used to induce focal cerebral ischemia in rats (n=48). All animals underwent sequential MRI and FDG positron emission tomography imaging at different times (30–150 minutes) after middle cerebral artery occlusion. MR and positron emission tomography images were coregistered. FDG uptake in the peri-ischemic zone was assessed in relation to middle cerebral artery occlusion duration, cerebral blood flow, apparent diffusion coefficient, and 24-hour T2 lesions.

Results—Elevated FDG uptake was consistently observed at the peri-ischemic zone surrounding the presumed ischemic core with low FDG uptake. Both the spatial volume and the uptake level of the hyper-uptake region were inversely correlated with the duration of middle cerebral artery occlusion. The hyper-uptake regions exhibited a mild reduction of cerebral blood flow (28.2±3.2%) and apparent diffusion coefficient (9.1±1.4%) when compared with that in the contralateral hemisphere. Colocalization analysis revealed that, with reperfusion, an average of 12.1±1.7% of the hyper-uptake volume was recruited into final infarction.

Conclusions—Elevated FDG uptake at the peri-ischemic zone is consistently observed during acute cerebral ischemia. The region with elevated FDG uptake likely reflects viable tissues that can be salvaged with reperfusion. Therefore, acute FDG positron emission tomography imaging might hold promise in the management of patients with acute stroke.

Keywords

acute ischemic stroke; cerebral glucose metabolism; FDG PET

© 2013 American Heart Association, Inc.

Correspondence to Weili Lin, PhD, Biomedical Research Imaging Center, University of North Carolina at Chapel Hill, CB# 7513, NC. weili_lin@med.unc.edu.

Disclosures
None.

The online-only Data Supplement is available with this article at http://stroke.ahajournals.org/lookup/suppl/doi:10.1161/STROKEAHA.113.000903/-/DC1.

NIH-PA Author Manuscript
NIH-PA Author Manuscript
NIH-PA Author Manuscript

NIH-PA Author Manuscript

NIH-PA Author Manuscript

NIH-PA Author Manuscript

During cerebral ischemia, reduction of cerebral blood flow (CBF) directly results in concurrent reduction of oxygen and glucose supply to the brain, which in turn leads to disturbed glucose metabolism and subsequent cellular dysfunctions attributed by the loss of ATP.[1,2] Depending on the extent to which CBF is reduced, alternations of glucose metabolism could vary both spatially and temporally. Specifically, it has been widely and consistently reported that glucose metabolism is greatly suppressed in the ischemic core because of severe flow reduction in animals and patients with stroke using either ^{14}C-2-deoxyglucose autoradiography[3,4] or positron emission tomography (PET) imaging with [^{18}]F-2-fluoro-2-deoxy-D-glucose (FDG).[5,6] In contrast, results on the spatial and temporal patterns of glucose metabolism in regions with moderate CBF reduction are somewhat inconsistent. Using autoradiography, increased glucose uptake was observed near the ischemic border 30 minutes and 1 hour after middle cerebral artery occlusion (MCAO) in animals.[3,7] However, Belayev et al[8] reported a heterogeneous distribution of usage of glucose in the peri-ischemic zone with sporadic loci of focally elevated or depressed glucose uptake 2 hours after MCAO in a rat ischemic stroke model. As a result, no significant quantitative changes were observed in glucose metabolism between the 2 hemispheres. Using PET, an increased uptake of FDG in regions with mild reduction of CBF was also reported in rats 75 minutes after MCAO.[9] However, this hyper-uptake pattern no longer existed 3 hours after MCAO in another study.[10] Nasu et al[11] imaged patients with stroke 1 to 7 days after cerebral ischemia using FDG PET, and hyper-accumulation of FDG was observed around the depressed uptake core in 7 of 20 patients. Collectively, although severely diminished glucose metabolism is consistently observed in ischemic core, characteristics of glucose uptake at the peri-ischemic zone remain controversial. Although several factors, including species, MCAO models, and imaging analysis approaches might contribute to the reported inconsistent FDG uptake patterns at the peri-ischemic regions, one of the most plausible explanations may be the different time intervals between the onset of MCAO and time of glucose metabolism assay or FDG PET imaging. Furthermore, studies investigating quantitative association between FDG hyper-uptake and final tissue outcome are lacking. To this end, this study aimed to characterize spatiotemporal glucose uptake patterns during acute cerebral ischemia using FDG PET in a rat MCAO model. Time intervals between FDG injection and onset of MCAO were varied ranging from 30 to 150 minutes after MCAO. FDG uptake in the peri-ischemic zone was assessed in relation to MCAO duration, CBF, and apparent diffusion coefficient (ADC) for all animals, and to 24-hour T2 lesions for reperfused animals. Delineation of the spatiotemporal characteristics of FDG uptake during acute ischemia may offer insights into dynamic alterations of glucose metabolism, which may shed light on tissue viability.

Methods

A total of 48 male Long Evans rats (Charles River, Wilmington, MA) weighing between 250 and 350 g were included. All animal protocols were approved by the Institutional Animal Care and Use Committee. Animals were divided into 5 groups on the basis of when FDG was injected in relation to MCAO onset time, including 30 (n=5), 60 (n=13), 90 (n=13), 120 (n=12), and 150 minutes (n=5) after MCAO. MRI were acquired first followed by PET imaging. A subset of animals (n=20) underwent reperfusion procedures (reperfusion subgroup hereafter) immediately after PET imaging to discern the potential relation between FDG uptake and final tissue fate. All the remaining animals not included in the reperfusion subgroup were euthanized for autoradiography. In the reperfusion subgroup, animals were again divided into 4 groups depending on when FDG was given, including 30, 60, 90, and 120 minutes after MCAO (n=5 for each subgroup). Reperfusion was accomplished immediately after 40-minute PET scans resulting in a MCAO duration of 70, 100, 130, and 160 minutes, respectively. Animals were MR imaged 24 hours after MCAO and were

NIH-PA Author Manuscript

NIH-PA Author Manuscript

NIH-PA Author Manuscript

euthanized after MRI. Detailed experimental protocols are provided in Figure I in the online-only Data Supplement.

Surgical Procedures

The intraluminal MCAO method was adopted to induce focal cerebral ischemia.[12] The suture was placed into the internal carotid artery via the external carotid artery stump and advanced for ≈21 mm until resistance was felt. For reperfusion, anesthesia was briefly discontinued when animals were transported from the PET scanner to the surgical table where isoflurane anesthesia was restored. Reperfusion was accomplished by withdrawing the suture from the internal carotid artery to the external carotid artery to restore blood flow. More information is provided in Surgical Procedures in the online-only Data Supplement.

Imaging

MRI were acquired using a Bruker 9.4T scanner (BioSpec 94/30; Bruker BioSpin, Inc, Billerica, MA) and a phased array surface coil. T1-weighted, T2-weighted (T2w), and echo planar imaging diffusion-weighted images were acquired and ADC maps were calculated. The dynamic susceptibility contrast approach using a single-shot echo planar imaging sequence was used and a singular value decomposition method was used for obtaining CBF maps.[13] All imaging parameters are provided in the online-only Data Supplement.

FDG PET imaging was performed using a small animal PET/computed tomography (CT) scanner (Vista eXplore, GE Healthcare, Inc) with a center resolution of 1.2- and 46-mm axial field of view.[14] A 7-minute CT scan was first acquired for subsequent attenuation correction and anatomic registration. FDG (39.4±8.2 MBq) diluted in saline was injected via the tail vein at the predefined time after MCAO. With the exception of the 30-minute group, dynamic PET acquisition was performed for 40 minutes (Figure I in the online-only Data Supplement). The list-mode PET data were binned 3×10, 3×30, 1×180, 3×300, and 2×600 s. For the 30-minute group, FDG was injected during MRI, and PET images were acquired for 10 minutes using the static acquisition mode. Data were reconstructed using the 2-dimensional ordered subset expectation–maximization algorithm with random, scatter, and attenuation correction.

Autoradiography

With the exception of the animals in the reperfusion subgroup, animals were euthanized after PET (Figure I in the online-only Data Supplement) and brain tissues were collected and snap-frozen in liquid nitrogen. Three coronal sections of 14 μm thickness were cut at 4, 5, and 6 mm below the brain anterior apex. Six of 28 animals had poor cutting qualities (wrinkles and tissue lost, etc.) and were excluded from the final analyses (more information is provided in Autoradiography in the online-only Data Supplement).

Image Analysis

All MRI from the same animals were first registered using the FLIRT[15] in FSK 3.2 (FMRIB, Oxford, United Kingdom). Skull bone structure was extracted from CT images using a threshold method. T1-weighted MRI were bias corrected and Hessian matrix filtered for sheet-like structure detection[16] to extract bony structures. The CT and MR bone images were registered using a rigid-body registration scheme. The transformation matrices were subsequently used to register all MRI onto CT images. PET images were registered to CT images using a mutual-information–based registration method.

FDG hyper-uptake volume (V_{hyper}) was obtained as the brain regions in the ipsilateral hemisphere that exhibited a standardized uptake value (SUV) level greater than the mean +2SD of that in the contralateral hemisphere from PET images that were taken 30 to 40

NIH-PA Author Manuscript

NIH-PA Author Manuscript

NIH-PA Author Manuscript

minutes after FDG injection. In addition, V_{hyper} fraction (F_{hyper}) was calculated as the V_{hyper} divided by the ipsilateral hemispheric volume. Similar criteria were applied on autoradiography images to obtain volume with hyper-FDG uptake and F_{hyper} averaged from 3 sections was calculated for each animal.

Ischemic core volume was manually traced from each animal in the reperfusion subgroup using the 24-hour T2w images. Volume measurements were obtained from 14 coronal slices of the registered PET or MRI (from bregma +3.7 mm to bregma −7 mm and 0.775 mm per slice) covering the MCA territory. Both the FDG hyper-uptake and ischemic core volumes were overlaid onto the corresponding registered CBF and ADC maps acquired before PET imaging of the same animal. Subsequently, the ratios of CBF and ADC in both the hyper-uptake and the ischemic core regions to that of the homologous regions in the contralateral hemisphere were obtained for different MCAO groups, respectively. To determine the extent to which the FDG hyper-uptake regions were recruited into the infarction, an overlap volume ratio (OVR) was calculated as the ratio of the overlap volume between V_{hyper} and infraction to V_{hyper}.

Statistical Analysis

Data are presented as mean±SEM unless specified. Differences across groups were compared using 1-way ANOVA for the F_{hyper} and SUV ratios. Multiple comparisons between groups were made using the Bonferroni test. Normality test was passed for all data sets. Pearson correlation analysis was performed using GraphPad Prism software. $P<0.05$ was considered significant.

Results

The exact time intervals between MCAO and FDG injection for the 5 groups were 30 minutes (35.6±7.1 minutes), 60 minutes (60.8±9.0 minutes), 90 minutes (88.2±4.9 minutes), 120 minutes (124.7±7.3 minutes), and 150 minutes (153.6±5.9 minutes), respectively. Spatiotemporal dynamics of FDG uptake of a representative rat is shown in Figure 1. A brain region with extremely low FDG uptake is clearly visible shortly after FDG injection, most likely reflecting the ischemic core. An elevated FDG uptake region (arrows) becomes visible 1200 s and more apparent 1800 s after FDG injection, which continues to increase throughout the PET imaging session. Regardless of MCAO durations, averaged time uptake curves (Figure 1, bottom) demonstrate that the hyper-uptake region always exhibits a lower FDG uptake initially but continuously increases, surpasses normal tissue at around 10 to 20 minutes, and reaches significant differences at 30 to 40 minutes after injection.

The spatial characteristics of FDG uptake in relation to MCAO duration are shown in Figure 2. Evidently, a larger V_{hyper} is observed in animals with a shorter MCAO duration when compared that with a longer MCAO duration (Figure 2A). Specifically, F_{hyper} is inversely correlated with MCAO duration (Figure 2B; $r=-0.62$; $P<0.001$). Similarly, an inverse relationship also exists between the SUV ratio of the hyper-uptake and normal-uptake regions and the MCAO duration with an r of −0.46 (Figure 2C; $P<0.05$). Similar findings as those using PET are also observed using autoradiography (Figure 3), where the F_{hyper} - is inversely correlated with the MCAO duration ($r=-0.45$; $P<0.05$), further confirming the validity of the PET findings.

The extent of ischemic injury in the hyper-FDG uptake regions was evaluated in the context of ADC and CBF reduction (Figure 4). The ischemic core exhibits 71.9±1.0% and 32.5±0.7% reduction of CBF and ADC, respectively (averaged from animals in the reperfusion subgroup), whereas the hyper-FDG uptake regions show 28.2±3.2% CBF and 9.1±1.4% ADC reductions (averaged from all animals), suggesting less severe ischemic

NIH-PA Author Manuscript

NIH-PA Author Manuscript

NIH-PA Author Manuscript

injury in this region when compared with that in the ischemic core. In addition, the extent to which ADC and CBF is reduced in both the hyper-FDG uptake regions and the ischemic core seems independent of MCAO durations among the 5 groups (P>0.05).

The OVR (Figure 5) measured from animals in the reperfusion subgroup is small (Figure 5B) and statistically not different among groups (16.0±5%, 12.7±2.8%, 10.7±3.1%, and 9.1±2.9% for 30, 60, 90, and 120 minutes groups, respectively; P=0.55), leading to an overall average OVR of 12.1±1.7% from all animals in the reperfusion subgroup. In addition, the 24-hour T2 lesion, the F_{hyper}, and the overlap volumes (mm^3) are provided in the Figure II in the online-only Data Supplement. These results demonstrate that the majority of the FDG hyper-uptake tissue was not recruited into 24-hour T2w lesion. Additional boundary analysis to determine the spatial relation between regions of FDG hyper-uptake and 24-hour T2 lesion is provided in Table I in the online-only Data Supplement.

Discussion

Spatiotemporal dynamics of FDG uptakes during acute cerebral ischemia were evaluated in a MCAO rat model. In addition to the anticipated reduction of FDG uptake in the ischemic lesions, an elevated FDG uptake is present at the peri-ischemic regions, consistent with that observed using autoradiography. The F_{hyper} inversely correlates with the duration of MCAO (Figure 2), suggesting that the spatial extent of the observed elevated FDG uptake may be modulated by the severity of ischemic injury. Temporally, independent of time interval between MCAO and FDG injection, the SUV in the hyper-uptake regions surpasses the normal brain area 10 to 20 minutes after FDG injection and persists throughout the remaining PET imaging session (Figure 1). Mild reductions of CBF and ADC are found in the hyper-uptake regions when compared with that in the contralateral hemisphere (Figure 4). More importantly, the majority of the hyper-FDG uptake volume is not recruited into infarction in the reperfused animals (Figure 5), suggesting that the hyper-FDG uptake regions may represent viable tissue that can be salvaged after reperfusion.

Although an increased accumulation of glucose around the ischemic border was first reported by Ginsberg et al[3] in 1977 using 2-deoxy- D-glucose in a 60-minute MCAO cat model, this finding has not been consistently observed in subsequent reports by other groups.[8–10] We postulate that the discrepancy of time intervals between MCAO onset and assessments of brain glucose metabolism among the reported studies can be the major factor contributing to the inconsistent findings in the literature. Although our results suggest that the hyper-FDG uptake at the peri-ischemic region is consistently observed between 30 and 150 minutes after MCAO, an inverse relation between F_{hyper} and time is observed. This finding suggests that (1) beyond 150 minutes after MCAO, the volume of hyper-FDG uptake is small and (2) imaging spatial resolution can be essential to delineate the presence or the absence of hyper-FDG uptake. Specifically, a dedicated high-resolution animal PET system was not available until recently. Therefore, it is conceivable that hyper-FDG uptake in the peri-ischemic region was present, but the lack of dedicated small animal PET prevented it from conclusively observed.

Several potential mechanisms may account for the observed hyper-uptake FDG in the peri-ischemic zone. Using a permanent MCAO rat model and FDG PET, Schroeter et al[17] found increased glucose metabolism and concurrently increased neuroinflammation (PK-11195 PET) in the peri-ischemic regions 7 days after stroke. Similarly, Fukumoto et al[18] reported neuroinflammation-related hyper-FDG uptake 7 days after photothrombosis ischemia but not before day 7. However, inflammation processes are unlikely to explain findings in our study because PET images were obtained within 30 to 150 minutes after MCAO when

NIH-PA Author Manuscript

NIH-PA Author Manuscript

NIH-PA Author Manuscript

significant neuroinflammation is not expected. The expression of glial fibrillary acidic protein only starts to increase its mRNA 6 hours after occlusion in rats[19] and transmigration of blood-borne leukocytes is expected in more delayed phases of ischemic injury. Alternatively, our results may suggest an elevated glycolysis at the peri-ischemic regions during acute cerebral ischemia to compensate the loss of ATP. Lactate bioluminescence imaging showed a higher lactate content in regions similar to the elevated FDG uptake area, indicating glucolytic glucose metabolism in this area (Lactate bioluminescence imaging; Figure III in the online-only Data Supplement). Whether this increased glucose metabolism represents aerobic or anaerobic glycolysis is still under debate. Several early studies attributed the increased glucose accumulation in the peri-ischemic region to anaerobic glycolysis;[20,21] however, other studies seem to argue against this conclusion. Wise et al[5] conducted a serial PET study with measurements of both oxygen cerebral metabolic rate (CMR) and cerebral glucose metabolic rate (CMRglu) in patients with stroke 1 to 31 days after stroke. They found a lower oxygen extraction in the ischemic lesion, meaning adequate oxygen supply, and the ratio of oxygen consumption and glucose metabolism was only one third of that in normal brain tissue, indicating aerobic rather anaerobic glycolysis in recovering ischemic tissue.[5] In our study, only mild reduction of CBF was found in the observed hyper-uptake regions, suggesting certain availability of oxygen in those regions, and thus possible aerobic glycolysis, the conversion of glucose to lactate in the presence of oxygen. Even though glycolysis is not energy efficient, it might be effective in protecting cells from depolarizing because of its fast turn-around rate and its role as a membrane energy provider.[22] Therefore, it is possible that cells near the peri-ischemic zone use aerobic glycolysis as the main energy production source to meet major cellular needs.

It is worth noting that elevated FDG uptake in the peri-ischemic region might not be equivalent to increased glucose metabolism because of potential alteration of the lumped constant (LC). The LC is the ratio between FDG and glucose metabolic rates, accounting for differences of transportation, phosphorylation, and volume of distribution between these 2 compounds.[23] Although Hawkins et al[24] reported that there were no or very small LC variations between ischemic and nonischemic tissues, more recent studies seem to suggest a significant increase of the LC in ischemic or hypoperfused tissues, ranging from 20% to 78%.[25,26] Additional studies will be needed to further determine whether regional LC changes are present in the MCAO model used in our study.

The majority of the peri-ischemic regions exhibiting elevated FDG uptake seems to survive in the reperfused animals (Figure 5), suggesting that acute PET imaging may offer insights into tissue viability during cerebral ischemia. Specifically, a comprehensive study determining the relation among CBF, CMRglu, ATP, and nicotinamide adenine dinucleotide in a gerbil stroke model was conducted by Paschen et al.[27] A 2-fold increase of CMRglu above the normal level was observed for CBF between 20 and 35 mL/min per 100 g but declined sharply for CBF <20 mL/min per 100 g. More importantly, the CBF threshold for CMRglu reduction coincided with the initial ATP reduction as CBF decreased. Paschen et al[27] thus concluded that tissues with an increased CMRglu during acute cerebral ischemia may represent penumbral tissues. Our findings seem highly consistent with that reported by Paschen et al.[27] In addition to the fact that only a small fraction of the hyper-uptake regions was recruited into infarction, the inverse relation between F_{hyper} and the SUV ratio and the MCAO duration is also consistent with the anticipated reduction of penumbral volume with MCAO duration. Nevertheless, there are several fundamental methodological differences between their and our studies. In particular, FDG uptake might not fully represent CMRglu. Future studies focusing on the potential usage of CMRglu may be warranted.

Notice our experimental protocol, the FDG was given at a fixed time in relation to reperfusion (40 minutes prior) independent of MCAO duration (Figure I in the online-only

NIH-PA Author Manuscript

NIH-PA Author Manuscript

NIH-PA Author Manuscript

Data Supplement). This experimental design most likely leads to the observed relatively stable OVR across groups (Figure 5). A future alternative approach to further confirm our current findings is to administer FDG at a fixed time in relation to the onset of MCAO, that is, at 30 minutes after MCAO, followed by PET imaging, while varying the durations of MCAO before reperfusion across different animals. In so doing, one would expect a positive correlation between OVR and MCAO duration.

Our study also consists of 2 major shortcomings. First, it has been demonstrated that infract volume may continue to grow beyond the first 24 hours after reperfusion,[28] raising a question as to whether 24-hour T2w lesion reflects the final infarction. To address this question, a pilot study (n=5) was conducted where T2 lesion was assessed in the same animals 24 and 48 hours after reperfusion. Although our result shows a small increase of T2 lesion volume, 5.1±1.8%, from 24 to 48 hours after MCAO (Figure IV in the online-only Data Supplement), it should be noted that continuing lesion growth may be present. Second, brain swelling resulting from brain edema may be present in the 24-hour T2w images, leading to potential confounds when acute PET images were registered with the 24-hour T2w images using rigid registration algorithms. Correcting the effects of edema using approaches proposed by either Leach et al[29] or Swanson et al[30] may not be effective for the spatial overlay analysis used in this study because these methods rely on volume comparison between the 2 hemispheres. A more appropriate method may be the deformable registration approach. However, deformable registration for MR and PET is complex and the accuracy of different deformable registration approaches in animals is yet to be determined.

In conclusion, spatiotemporal characteristics of FDG uptake in an acute MCAO ischemic stroke rat model were revealed. In addition to the well anticipated reduction of FDG uptake in the ischemic lesions, hyper-FDG uptake at the peri-ischemic regions is consistently observed. This hyper-FDG uptake area may represent viable tissue because most of the hyper-uptake regions were not recruited into the infarction. Future work will focus on validating whether the region of hyper-FDG uptake is indeed ischemia penumbra by further extending MCAO >150 minutes and including a permanent occlusion model. Considering the wide availability of FDG PET imaging capability in most of the medical centers, our results underscore the potential clinical usage of FDG PET in the management of patients with acute stroke.

Supplementary Material

Refer to Web version on PubMed Central for supplementary material.

Acknowledgments

Sources of Funding

The work was supported by National Institutes of Health (3R01NS054079-04S).

The authors thank the UNC BRIC Small Animal Imaging Facility for imaging support and Dr Schroeder from the Department of Radiation Oncology, Duke University Medical Center, for helps on the lactate bioluminescence study.

References

1. Ginsberg MD, Belayev L, Zhao W, Huh PW, Busto R. The acute ischemic penumbra: topography, life span, and therapeutic response. Acta Neurochir Suppl. 1999; 73:45–50. [PubMed: 10494340]
2. Heiss WD. The ischemic penumbra: correlates in imaging and implications for treatment of ischemic stroke. The Johann Jacob Wepfer award 2011. Cerebrovasc Dis. 2011; 32:307–320. [PubMed: 21921593]

NIH-PA Author Manuscript
NIH-PA Author Manuscript
NIH-PA Author Manuscript

3. Ginsberg MD, Reivich M, Giandomenico A, Greenberg JH. Local glucose utilization in acute focal cerebral ischemia: local dysmetabolism and diaschisis. Neurology. 1977; 27:1042–1048. [PubMed: 22053]
4. Belayev L, Busto R, Zhao W, Clemens JA, Ginsberg MD. Effect of delayed albumin hemodilution on infarction volume and brain edema after transient middle cerebral artery occlusion in rats. J Neurosurg. 1997; 87:595–601. [PubMed: 9322848]
5. Wise RJ, Rhodes CG, Gibbs JM, Hatazawa J, Palmer T, Frackowiak RS, et al. Disturbance of oxidative metabolism of glucose in recent human cerebral infarcts. Ann Neurol. 1983; 14:627–637. [PubMed: 6606390]
6. Baron JC, Rougemont D, Soussaline F, Bustany P, Crouzel C, Bousser MG, et al. Local interrelationships of cerebral oxygen consumption and glucose utilization in normal subjects and in ischemic stroke patients: a positron tomography study. J Cereb Blood Flow Metab. 1984; 4:140–149. [PubMed: 6609928]
7. Robertson CA, McCabe C, Gallagher L, del Lopez-Gonzalez MR, Holmes WM, Condon B, et al. Stroke penumbra defined by an MRI-based oxygen challenge technique: 1. Validation using [14C]2-deoxyglucose autoradiography. J Cereb Blood Flow Metab. 2011; 31:1778–1787. [PubMed: 21559032]
8. Belayev L, Zhao W, Busto R, Ginsberg MD. Transient middle cerebral artery occlusion by intraluminal suture: I. Three-dimensional autoradiographic image-analysis of local cerebral glucose metabolism-blood flow interrelationships during ischemia and early recirculation. J Cereb Blood Flow Metab. 1997; 17:1266–1280. [PubMed: 9397026]
9. Walberer M, Backes H, Rueger MA, Neumaier B, Endepols H, Hoehn M, et al. Potential of early [(18)F]-2-fluoro-2-deoxy-D-glucose positron emission tomography for identifying hypoperfusion and predicting fate of tissue in a rat embolic stroke model. Stroke. 2012; 43:193–198. [PubMed: 22033990]
10. Sobrado M, Delgado M, Fernández-Valle E, García-García L, Torres M, Sánchez-Prieto J, et al. Longitudinal studies of ischemic penumbra by using 18F-FDG PET and MRI techniques in permanent and transient focal cerebral ischemia in rats. Neuroimage. 2011; 57:45–54. [PubMed: 21549205]
11. Nasu S, Hata T, Nakajima T, Suzuki Y. Evaluation of 18F-FDG PET in acute ischemic stroke: assessment of hyper accumulation around the lesion. Kaku Igaku. 2002; 39:103–110. [PubMed: 12058418]
12. Belayev L, Alonso OF, Busto R, Zhao W, Ginsberg MD. Middle cerebral artery occlusion in the rat by intraluminal suture. Neurological and pathological evaluation of an improved model. Stroke. 1996; 27:1616–1622. discussion 1623. [PubMed: 8784138]
13. Oster gaard L, Weisskoff RM, Chesler DA, Gyldensted C. Rosen High resolution measurement of cerebral blood flow using intravascular tracer bolus passages. Part I: Mathematical approach and statistical analysis. Magn Reson Med. 1996; 36:715–725. [PubMed: 8916022]
14. Wang Y, Seidel J, Tsui BM, Vaquero JJ, Pomper MG. Performance evaluation of the GE healthcare eXplore VISTA dual-ring small-animal PET scanner. J Nucl Med. 2006; 47:1891–1900. [PubMed: 17079824]
15. Jenkinson M, Smith S. A global optimisation method for robust affine registration of brain images. Med Image Anal. 2001; 5:143–156. [PubMed: 11516708]
16. Koller TM, Gerig G, Szekely G. Multiscale detection of curvilinear structures in 2-d and 3-d image data. IEEE International Conference on Computer Vision. 1995; 6:864–869.
17. Schroeter M, Dennin MA, Walberer M, Backes H, Neumaier B, Fink GR, et al. Neuroinflammation extends brain tissue at risk to vital peri-infarct tissue: a double tracer [11C]PK11195- and [18F]FDG-PET study. J Cereb Blood Flow Metab. 2009; 29:1216–1225. [PubMed: 19352400]
18. Fukumoto D, Hosoya T, Nishiyama S, Harada N, Iwata H, Yamamoto S, et al. Multiparametric assessment of acute and subacute ischemic neuronal damage: a small animal positron emission tomography study with rat photochemically induced thrombosis model. Synapse. 2011; 65:207–214. [PubMed: 20665726]

NIH-PA Author Manuscript

NIH-PA Author Manuscript

NIH-PA Author Manuscript

19. Yamashita K, Vogel P, Fritze K, Back T, Hossmann KA, Wiessner C. Monitoring the temporal and spatial activation pattern of astrocytes in focal cerebral ischemia using in situ hybridization to GFAP mRNA: comparison with sgp-2 and hsp70 mRNA and the effect of glutamate receptor antagonists. Brain Res. 1996; 735:285–297. [PubMed: 8911667]
20. Kuhl DE, Phelps ME, Kowell AP, Metter EJ, Selin C, Winter J. Effects of stroke on local cerebral metabolism and perfusion: mapping by emission computed tomography of 18FDG and 13NH3. Ann Neurol. 1980; 8:47–60. [PubMed: 6967712]
21. Kita H, Shima K, Tatsumi M, Chigasaki H. Cerebral blood flow and glucose metabolism of the ischemic rim in spontaneously hypertensive BR. stroke-prone rats with occlusion of the middle cerebral artery. J Cereb Blood Flow Metab. 1995; 15:235–241. [PubMed: 7860657]
22. Pellerin L, Magistretti PJ. Excitatory amino acids stimulate aerobic glycolysis in astrocytes via an activation of the Na+/K+ ATPase. Dev Neurosci. 1996; 18:336–342. [PubMed: 8940604]
23. Phelps ME. Positron computed tomography studies of cerebral glucose metabolism in man: theory and application in nuclear medicine. Semin Nucl Med. 1981; 11:32–49. [PubMed: 6972094]
24. Hawkins RA, Phelps ME, Huang SC, Kuhl DE. Effect of ischemia on quantification of local cerebral glucose metabolic rate in man. J Cereb Blood Flow Metab. 1981; 1:37–51. [PubMed: 6976973]
25. Nakai H, Yamamoto YL, Diksic M, Worsley KJ, Takara E. Triple-tracer autoradiography demonstrates effects of hyperglycemia on cerebral blood flow, pH, and glucose utilization in cerebral ischemia of rats. Stroke. 1988; 19:764–772. [PubMed: 3376169]
26. Noll T, Mühlensiepen H, Engels R, Hamacher K, Papaspyrou M, Langen KJ, et al. A cell-culture reactor for the on-line evaluation of radiopharmaceuticals: evaluation of the lumped constant of FDG in human glioma cells. J Nucl Med. 2000; 41:556–564. [PubMed: 10716332]
27. Paschen W, Mies G, Hossmann KA. Threshold relationship between cerebral blood flow, glucose utilization, and energy metabolites during development of stroke in gerbils. Exp Neurol. 1992; 117:325–333. [PubMed: 1397169]
28. Neumann-Haefelin T, Kastrup A, de Crespigny A, Yenari MA, Ringer T, Sun GH, et al. Serial MRI after transient focal cerebral ischemia in rats: dynamics of tissue injury, blood-brain barrier damage, and edema formation. Stroke. 2000; 31:1965–1972. discussion 1972. [PubMed: 10926965]
29. Leach MJ, Swan JH, Eisenthal D, Dopson M, Nobbs M. BW619C89, a glutamate release inhibitor, protects against focal cerebral ischemic damage. Stroke. 1993; 24:1063–1067. [PubMed: 8100654]
30. Swanson RA, Morton MT, Tsao-Wu G, Savalos RA, Davidson C, Sharp FR. A semiautomated method for measuring brain infarct volume. J Cereb Blood Flow Metab. 1990; 10:290–293. [PubMed: 1689322]

NIH-PA Author Manuscript
NIH-PA Author Manuscript
NIH-PA Author Manuscript

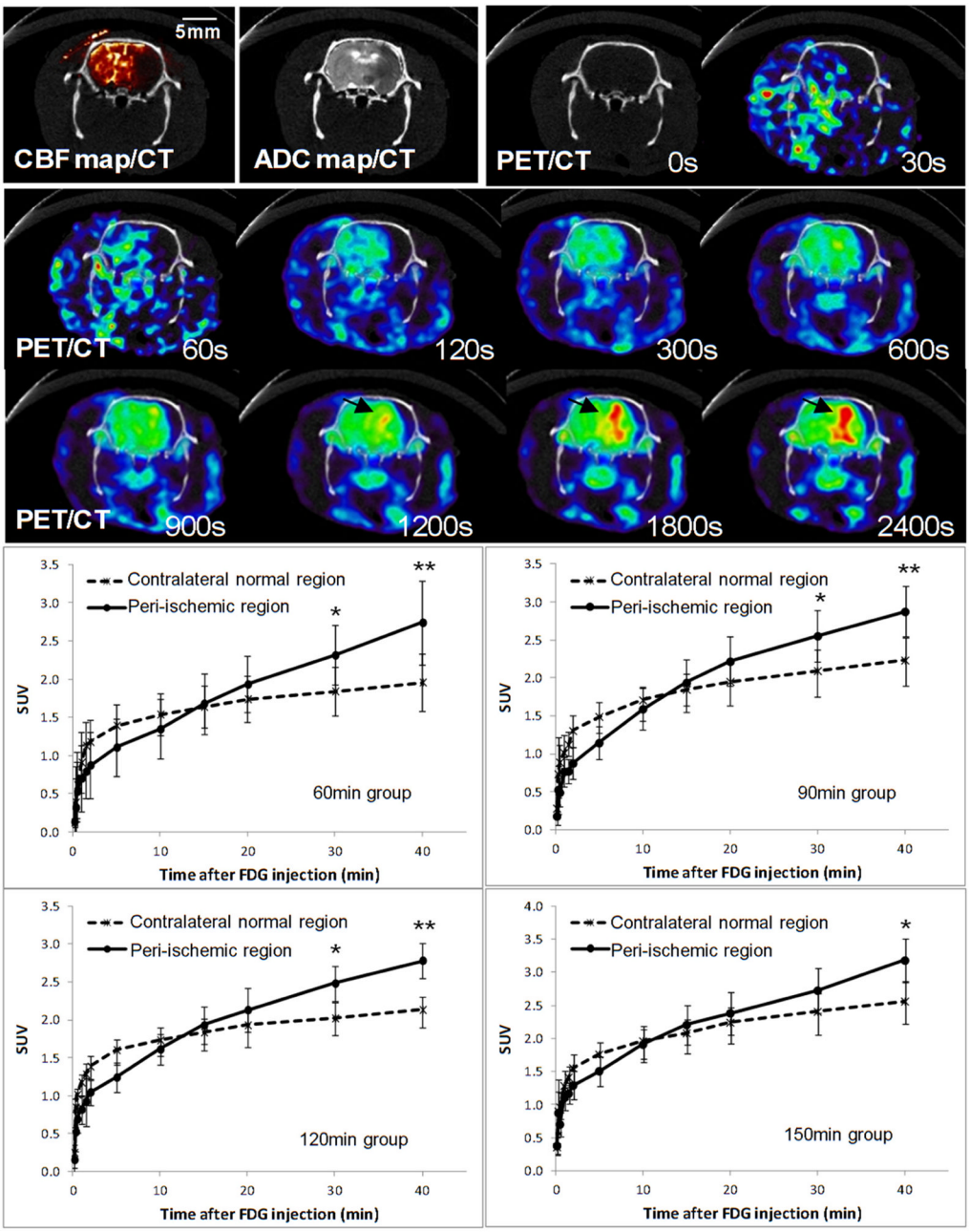

Figure 1.

Top, Coregistered cerebral blood flow (CBF) and apparent diffusion coefficient (ADC) maps superimposed on the computed tomographic (CT) images, and dynamic positron emission tomographic (PET) images from a rat with [^{18}]F-2-fluoro-2-deoxy-D-glucose (FDG) injected at 58 min after middle cerebral artery occlusion. Temporal and spatial FDG uptake distributions before (0 s) and after FDG injection (30–2400 s) are shown. Diminished FDG uptake in the right side of the brain indicates the ischemic lesion. Hyper-uptake of FDG (arrows) is clearly visible in the peri-ischemic region at 30 and 40 min. Dynamic uptake curves from a cortical region in the contralateral hemisphere (dashed lines) and peri-ischemic region (solid lines) are shown in the **bottom**. The peri-ischemic region was defined from the last PET frame showing elevated FDG uptake. FDG uptake in the peri-ischemic

region at 30 to 40 min after the injection was significantly higher than that in the contralateral hemisphere (**P<0.01; *P<0.05). SUV indicates standardized uptake value.

NIH-PA Author Manuscript
NIH-PA Author Manuscript
NIH-PA Author Manuscript

NIH-PA Author Manuscript

NIH-PA Author Manuscript

NIH-PA Author Manuscript

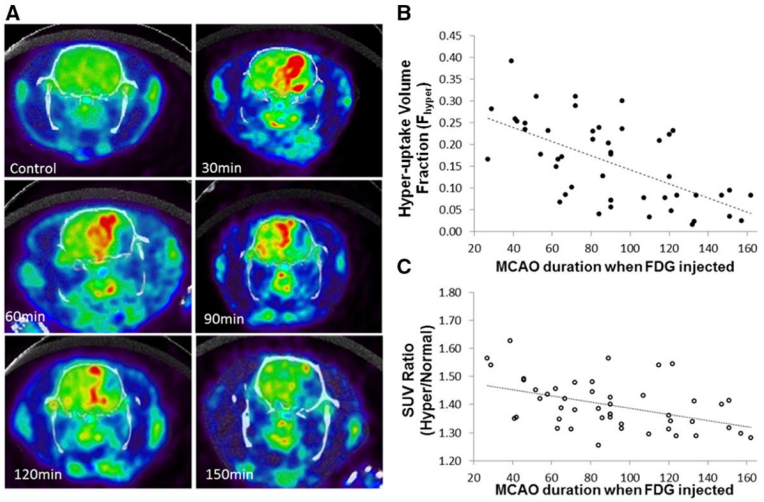

Figure 2.

A, [^{18}]F-2-fluoro-2-deoxy-D-glucose (FDG) positron emission tomographic (PET) images obtained from a control animal and a representative middle cerebral artery occlusion (MCAO) animal from each group with varied MCAO durations. PET images are overlaid on computed tomographic images. Scatter plots of hyper-uptake volume fraction (F_{hyper}; **B**) and standardized uptake value (SUV) ratios (**C**) reveal an inverse relation with MCAO duration. The dotted lines are the fitted linear regression lines.

NIH-PA Author Manuscript

NIH-PA Author Manuscript

NIH-PA Author Manuscript

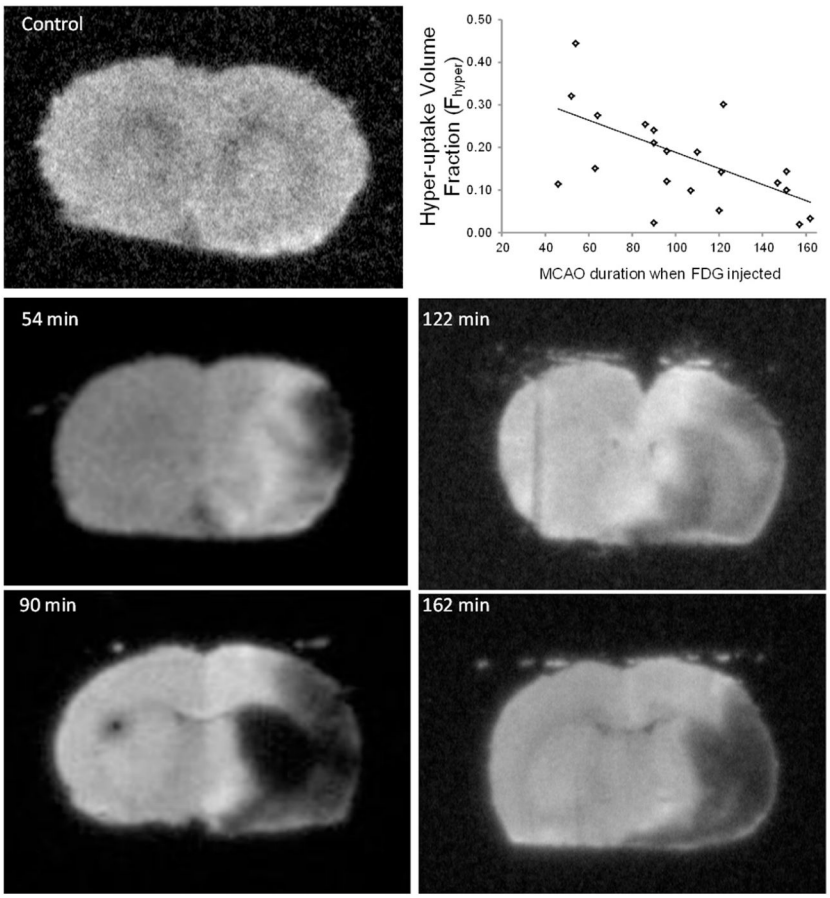

Figure 3.

High-resolution autoradiography images from a control and 4 representative middle cerebral artery occlusion (MCAO) rats demonstrate [^{18}]F-2-fluoro-2-deoxy-D-glucose (FDG) distribution in relation to MCAO duration. Time on the **upper left** corner of each image is the time interval between MCAO and FDG injection. The hyper-uptake volume fraction reduces as MCAO duration increases. The dotted line is the fitted linear regression line.

NIH-PA Author Manuscript

NIH-PA Author Manuscript

NIH-PA Author Manuscript

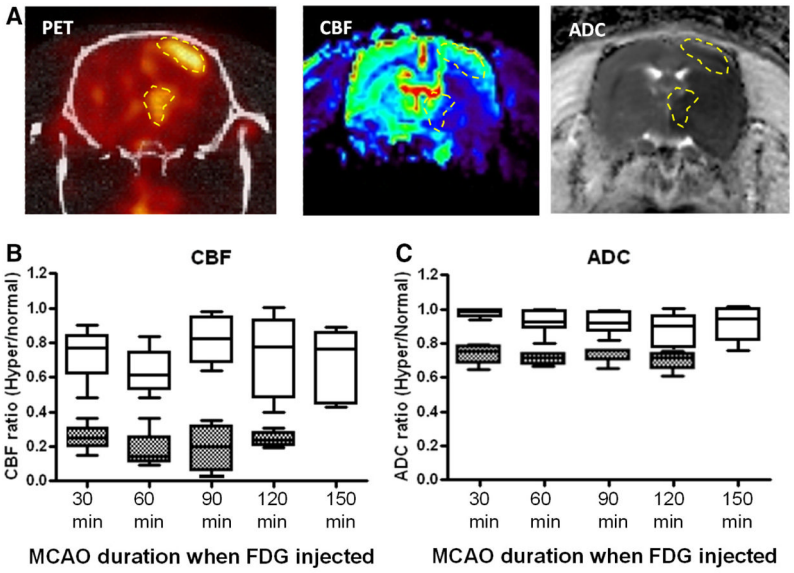

Figure 4.

A, Registered positron emission tomographic (PET)/computed tomographic, cerebral blood flow (CBF), and apparent diffusion coefficient (ADC) maps from a representative animal with [^{18}]F-2-fluoro-2-deoxy-D-glucose (FDG) injected at 120 min after middle cerebral artery occlusion (MCAO). Dotted lines indicate the regions with hyper-FDG uptake. The CBF (**B**) and ADC (**C**) ratios of the hyper-uptake tissue (□) or the ischemic core (▪) to the contralateral region are shown for different MCAO groups, respectively. Boxes indicate 75th and 25th percentile levels.

NIH-PA Author Manuscript

NIH-PA Author Manuscript

NIH-PA Author Manuscript

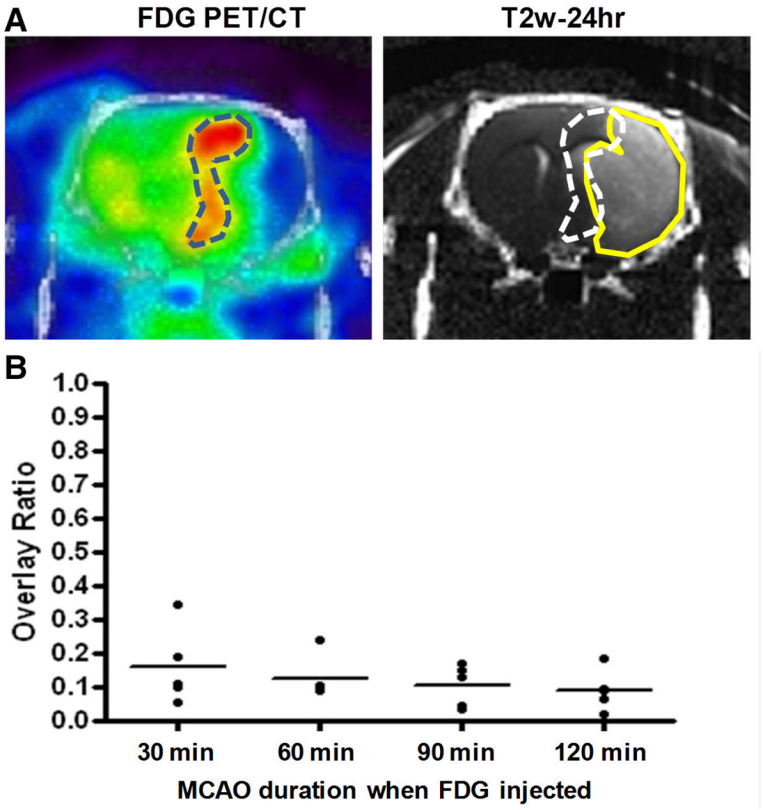

Figure 5.

Colocalization analysis on hyper-uptake and 24-h T2 lesion. **A**, An example of registered [^{18}]F-2-fluoro-2-deoxy-D-glucose (FDG) positron emission tomographic (PET)/computed tomographic (CT) and 24-h T2-weighted (T2w) images of a rat with FDG injected at 60 min after middle cerebral artery occlusion (MCAO) is shown (bregma +1.1 mm). The hyper-uptake region is marked by the dashed lines, whereas the 24-h T2 lesion is demarcated in yellow line. The overlap volume ratio (**B**) was measured from 14 coronal slides of registered images. Bars indicate mean overlap ratios for each group. No significant difference was found among the 4 groups.